

Mixing of MnPc electronic states at the MnPc/Au(110) interface

Cite as: J. Chem. Phys. **147**, 134702 (2017); <https://doi.org/10.1063/1.4996979>

Submitted: 20 July 2017 . Accepted: 14 September 2017 . Published Online: 03 October 2017

Pierluigi Gargiani, Simone Lisi, Giulia Avvisati, Pierluigi Mondelli, Sara Fatale, and Maria Grazia Betti



View Online



Export Citation



CrossMark

ARTICLES YOU MAY BE INTERESTED IN

[Spin switch in iron phthalocyanine on Au\(111\) surface by hydrogen adsorption](#)

The Journal of Chemical Physics **147**, 134701 (2017); <https://doi.org/10.1063/1.4996970>

[Electronic structure and bonding in metal phthalocyanines, Metal=Fe, Co, Ni, Cu, Zn, Mg](#)

The Journal of Chemical Physics **114**, 9780 (2001); <https://doi.org/10.1063/1.1367374>

[Electronic excitations of manganese phthalocyanine molecules](#)

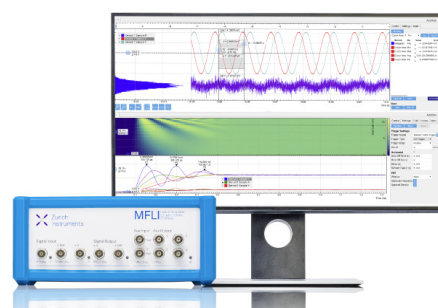
The Journal of Chemical Physics **148**, 044701 (2018); <https://doi.org/10.1063/1.5008916>

Challenge us.

What are your needs for periodic
signal detection?



Zurich
Instruments



Mixing of MnPc electronic states at the MnPc/Au(110) interface

Pierluigi Gargiani,^{a)} Simone Lisi,^{b)} Giulia Avvisati,^{c)} Pierluigi Mondelli, Sara Fatale, and Maria Grazia Betti

Dipartimento di Fisica, Università di Roma "La Sapienza," Piazzale A. Moro 5, I-00185 Roma, Italy

(Received 20 July 2017; accepted 14 September 2017; published online 3 October 2017)

Manganese-phthalocyanines form assembled chains with a variety of ordered super-structures, flat lying along the Au(110) reconstructed channels. The chains first give rise to a $\times 5$ symmetry reconstruction, while further deposition of MnPc leads to a $\times 7$ periodicity at the completion of the first single layer. A net polarization with the formation of an interface dipole is mainly due to the molecular π -states located on the macrocycles pyrrole rings, while the central metal ion induces a reduction in the polarization, whose amount is related to the Mn-Au interaction. The adsorption-induced interface polarization is compared to other $3d$ -metal phthalocyanines, to unravel the role of the central metal atom configuration in the interaction process of the d -states. The MnPc adsorption on Au(110) induces the re-hybridization of the electronic states localized on the central metal atom, promoting a charge redistribution of the molecular orbitals of the MnPc molecules. The molecule-substrate interaction is controlled by a symmetry-determined mixing between the electronic states, involving also the molecular empty orbitals with d character hybridized with the nitrogen atoms of the pyrrole ring, as deduced by photoemission and X-ray absorption spectroscopy exploiting light polarization. The symmetry-determined mixing between the electronic states of the Mn metal center and of the Au substrate induces a density of states close to the Fermi level for the $\times 5$ phase. *Published by AIP Publishing.* <https://doi.org/10.1063/1.4996979>

I. INTRODUCTION

A fascinating perspective in nanoscale systems is to investigate the assembling of molecular size-selected long range ordered two-dimensional (2D) structures, to precisely describe and control the molecular building block assembly and the interaction process with the underlying template.¹ Supramolecular assembly of metal-organic molecules on metallic substrates can be a convenient way for building up regular arrays exploiting the nano-patterning of suitable substrates, e.g. reconstructed channels² or vicinal surfaces.³ The controlled adsorption on the surface can lead to long-range ordered architectures with exotic electronic and magnetic properties, in the perspective of engineering nanoscale structures exploitable for nanoelectronics or spintronic devices.⁴

Metal-phthalocyanines (MPcs) are planar π -conjugated molecules with a central metal ion, which can be regularly assembled onto a naturally patterned surface.² Hybrid metal-organic interfaces with transition MPcs have been attracting interest thanks to their dual nature. In these molecules, a metal of the $3d$ series (i.e. Mn, Fe, Co, Ni, Cu, and Zn) is embedded in a π -conjugated organic cage and the organic macrocycles foster ordered arrays of regularly spaced metallic atoms firmly anchored to the surface, ensuring high thermal stability. The

central metal ion may give rise to intriguing properties, such as stable ferromagnetic phases obtained by stabilizing the metal-metal super-exchange coupling by means of the delocalized organic orbitals.⁵

Manganese phthalocyanines (MnPcs) are ferromagnetic molecular magnets in the solid- β -phase below 8.6 K,⁶ the highest Curie temperature among MPcs. The magnetic response is driven by a super-exchange interaction between the nearest neighbouring Mn atoms via π -orbitals on the Pc ring.^{7–10} The adsorption of MPcs on metal surfaces can alter their magnetic state due to the formation of new ligand bonds and the hybridization of molecular and substrate states,^{2,11–14} thus affecting the electronic and magnetic coupling of the metal ion to the substrate.^{15–17}

Understanding the change in chemical coordination and the electronic-state re-hybridization process is a preliminary step to achieve a full control over the functionality of these molecular systems adsorbed on surfaces. In particular, the chemical bond of the adsorbed molecule to the underlying surface can induce the redistribution of charge in the d orbitals of the metal center, modifying the ligand field of the metal ion and leading to a strong modification of the magnetic ground state (GS) of the system, as discussed for FePc, CoPc, and CuPc adsorbed on the Au(110) reconstructed channels.¹⁵

The interrelationship between the magnetic state and the symmetry of the involved orbitals is a key point to understand the interaction process. In the MnPc-Au(110) interaction, not only the central metal atom but also the pyrrole rings are involved in the process.¹⁸ Furthermore,

^{a)}Present address: ALBA Synchrotron Light Source, Carretera BP 1413, Km. 3.3 E-08290 Cerdanyola del Vallès, Barcelona, Spain.

^{b)}Present address: Institut Néel CNRS/UGA UPR2940, 25 Rue des Martyrs BP 166, 38042 Grenoble Cedex 9, France.

^{c)}Electronic mail: giulia.avvisati@uniroma1.it

polarization, dipoles at the interfaces, and charge transfer effects can induce a substantial charge redistribution, influencing the transport response at the organic-metal interfaces. In this paper, the interaction strength, the molecular orbital mixing, and the polarization effects of MnPc chains on Au(110) will be unraveled and then compared with the single layer (SL) formed by other 3d-metal phthalocyanines on the same Au template.

A. Experimental details

X-ray and high-resolution ultraviolet photoemission measurements were performed at the LOTUS laboratory, Sapienza University of Rome, in two different ultra-high-vacuum (UHV) chambers equipped with a low-energy electron diffraction (LEED) setup and the needed ancillary facilities for sample preparation. UV radiation is generated by means of the VG Scienta VUV 5050 photon source, with a monochromatized HeI_{α} ($h\nu = 21.218$ eV) spectral line. The photoemitted electrons were analyzed in the incidence plane with a hemispherical analyzer (Scienta SES-200) and angular integration has been performed over $\pm 8^\circ$ around normal emission. The work function (WF) change was determined by measuring the energy shift of the low-energy photoemission cutoff signal applying a -9 V bias to the sample with respect to ground. The X-ray photoemission spectra (XPS) were acquired impinging the sample with $Al K_{\alpha}$ radiation (1486.6 eV) and collecting the normally emitted photoelectrons with a VG Microtech Clam-2 hemispherical analyzer.

Near-edge X-ray absorption fine-structure (NEXAFS) measurements at the N K and Mn $L_{2,3}$ edges were performed at the ALOISA beamline of the ELETTRA synchrotron radiation facility. The spectra were acquired with a photon incidence angle of 87° switching the electric field polarization direction from parallel (in-plane) to normal (out-of-plane) to the sample surface. The potential damages due to exposure to X-ray beams were avoided by monitoring the C and N 1s core level before and after NEXAFS measurements.

A long-range ordered (1×2) reconstruction characterized by sharp LEED spots of the clean Au(110) surface was obtained by means of a double step sputtering-annealing treatment. The Au(110) surface was first Ar^+ -bombarded at the sputtering energy of 1 keV and then heated up to 725 K while, in the second cycle, the ion bombarding energy was lowered to 0.5 keV with an annealing temperature of 530 K. The Au(110)- 1×2 surface is characterized by a missing-row type reconstruction with atomic channels oriented along the $[1\bar{1}0]$ direction.

The MnPc deposition is obtained by evaporation from quartz crucibles of purified molecular powder with a deposition rate ($2.0 \text{ \AA}/\text{min}$) estimated by means of a quartz microbalance. The deposition of MnPc on the Au(110) surface was achieved by keeping the substrate at two different temperatures. Respectively, thick films are obtained with MnPc deposition on the surface kept at room temperature, while 2D ordered self-assembled structures are favored by keeping the substrate at 415 K during MnPc deposition. The completion of the first SL corresponds to the molecules arranged in a $\times 7$ phase, as observed by a clear change in the slope of the work

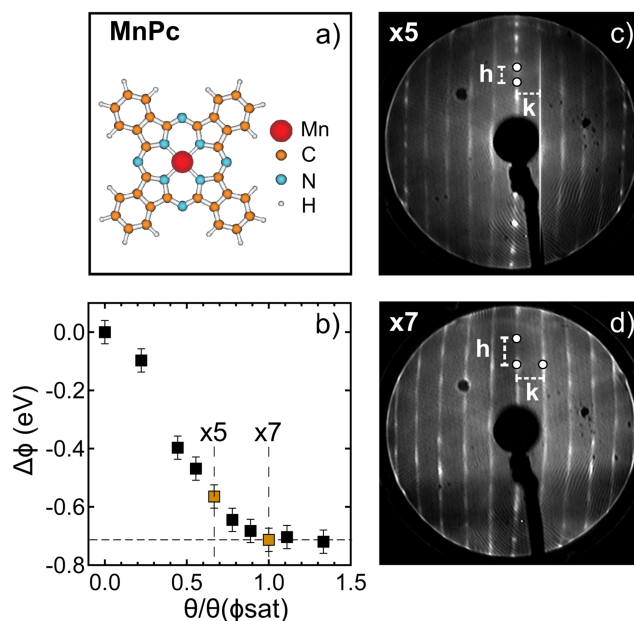


FIG. 1. (a) A sketch of the MnPc molecule. (b) Work function variation, with respect to clean Au(110), as a function of MnPc coverage up to the saturation level, corresponding to the single layer completion with a 5×7 reconstructed symmetry. [(c) and (d)] LEED pattern corresponding to a ($\times 5$) and a ($\times 7$) reconstructed surface, respectively, as deduced by the h/k ratio measured on the diffraction pattern. MnPc deposited on the Au(110) substrate kept at $T = 413$ K, LEED data acquired at $T = 80$ K, to avoid damages of the MnPc adlayer, with a primary beam energy of 50 eV.

function [see Fig. 1(b)] and confirmed by the quenching of the Au surface states in the valence band.

II. RESULTS

A. Long-range ordering and growth morphology

A selected set of LEED patterns for MnPc deposited on Au(110), at increasing molecular coverage, is reported in Fig. 1 (right panels). MnPc molecules, deposited on the Au(110)- 1×2 channels, promote new $\times 5$ and $\times 7$ reconstructions with n -fold periodicity dependent on the molecular density, as observed for other MPc molecules adsorbed on Au(110) (see, for example, Refs. 2, 19, and 20). The diffraction patterns are characterized by defined spots along the k direction, perpendicular to the substrate channels, showing $\times 5$ and $\times 7$ symmetry, upon increasing MnPc coverage. The fivefold substrate reconstruction ($a_{\times 5} = 14.4 \text{ \AA}$) corresponds to a unit cell fitting with the size of the MnPc molecule (13.8 \AA), suggesting an adsorption geometry similar to other MPcs on Au(110): flat-lying and lined up edge-to-edge along the $[1\bar{1}0]$ direction of the Au reconstructed channels.^{2,21,22} Parallel chains are not coherently aligned since faint elongated signals are detected in the h direction [Figs. 1(c) and 1(d)]. The distance between the axes of two adjacent chains is determined by the substrate reconstruction.^{2,19,21} Following the hypothesis that the MnPc molecular chain geometry replicates the adsorption of other MPcs on Au(110), the overall molecular density on the surface is 3.3×10^{-3} molecule per \AA^2 for the $\times 5$ phase, corresponding to well-oriented MnPc chains lying inside the Au(110) reconstructed channel, as reported in Ref. 22. Further increasing the molecular coverage induces a structural transition

leading to a $\times 7$ reconstruction, as can be deduced by the larger k -spacing between diffracted spots in Fig. 1(d). Even in this case, long-range order is maintained along the chains preserving a 2.9×5 Å lattice parameter. The 5-fold and 7-fold symmetry, observed for MPcs adsorbed in the Au(110) channels, has been attributed to a molecule-induced reconstruction of the plastic Au(110) surface, as observed for FePc² and CuPc²³ adsorbed on Au(110).

The molecular density can be estimated considering the superposition of two cells, as large as $(7 \times 4.1) \times (5 \times 2.9)$ Å², associated with the chains in the channels and on top of the gold rails.^{2,21} The total density amounts to 4.9×10^{-3} molecules/Å², in perfect agreement with the structural data reported in Ref. 22. Considering the close packed $\times 7$ configuration as the SL, the $\times 5$ phase can be evaluated at about 0.7 SL coverage.

The completion of a single compact molecular layer is reflected by the WF variation ($\Delta\Phi$) [Fig. 1(b)], with respect to the clean Au(110) substrate value, as a function of MnPc molecular density. The WF monotonically decreases down to a plateau at a value of $\Delta\Phi = -0.70$ eV that corresponds to the formation of the $\times 7$ phase. The $\times 5$ phase, corresponding to a surface reconstruction with a not completely covered Au substrate,² does not lead to discontinuity of the WF variation.

For all 3d-metal-phthalocyanines, a decreasing drop in the WF at the initial stage of deposition is observed. The experimental saturation values for MPcs with different 3d central metal atoms^{11,19} are reported in Table I. The work function decreasing upon the adsorption of π -conjugated molecules on metal surfaces has often been observed and it is generally attributed to the highly polarizable electrons located in the macrocycles, caused by the π electrons approaching on the surface.^{12,24}

In metal-organic interfaces, the interpretation of the energy level diagram and accordingly of the WF evolution is more complex with respect to inorganic interfaces. The latter are characterized by an interface dipole that can be easily defined, while metal-organic interfaces are affected by several concomitant processes, which are difficult to discern and interpret. Indeed, different parameters have to be considered, like polarization effects due to molecular dipoles, Pauli repulsion, screening effects, and molecular deformation.^{25,26} The reduction of the metal WF at the interface is due to the compression of the metal electron tails and due to polarization effects, while the interaction with the central metal atom of the molecules influences the WF with an amount

depending on the net charge transfer from the underlying metallic substrate to the 3d-orbitals of the molecule central metal ion.

The saturation values reveal that the work function variation is lower for less filled 3d shells of the central metal ion. For MPcs with 3d-metal partially filled molecular orbitals (i.e., MnPc, FePc, and CoPc), the polarization effects due to the π orbitals-substrate mixing are counterbalanced by a charge donation from the Au states to the central metal atom orbitals, determining a lower work function saturation value. This effect is maximum for MPc with a lower 3d metal orbital occupancy, where the interaction process can involve different 3d orbitals. The MnPc molecule has three unpaired electrons localized on the d_{xy} , d_{xz+yz} , and d_{z^2} orbitals that can contribute to the interaction with the substrate, allowing for a larger charge transfer with respect to the sequence of 3d-MPc molecules, determining the WF values reported in Table I. This larger substrate-molecule charge donation counterbalances the work function decreasing due to the polarization effects and Pauli repulsion, common to all MPcs deposited on metal surfaces, explaining the lower decrease observed for MnPc. A similar charge donation/back-donation process has been proposed to explain the interaction mechanism of CoPc/Ag(111)¹³ and MnPc/Ag(111).¹⁴

The molecular adsorption geometry for aligned MPc molecules on Au(110) is flat-lying on the Au channels, as can be confirmed by absorption spectra at the N K-edge of MnPc. NEXAFS data for the $\times 5$ configuration and for a thick molecular film (TF) of MnPc grown on the Au(110) surface are shown in Fig. 2. Nitrogen K edges are acquired with linearly polarized radiation, with the electric field vector either parallel (black curve) or almost normal (3° off, red curve) to the surface plane. The spectra present multiple absorption peaks associated with transitions from the N 1s core level to the empty states located on the pyrrole macrocycles, mainly of π^* symmetry, in the 399-406 eV energy region, and of σ^* character, above 406 eV. The dichroic response observed for the $\times 5$ phase (Fig. 2 bottom panel) is a consequence of the flat-lying adsorption configuration of the molecules along the Au(110) channels, similarly to MPcs with a different central metal atom on the

TABLE I. WF variation for a SL of MPc molecules with different central metal atoms (M = Mn, Fe, Co, Ni, Cu, Zn) self-assembled on Au(110).^{11,19}

MPc	$\Delta\Phi$ (eV)
MnPc	-0.70
FePc	-0.79
CoPc	-0.83
NiPc	-0.90
CuPc	-0.95
ZnPc	-0.95

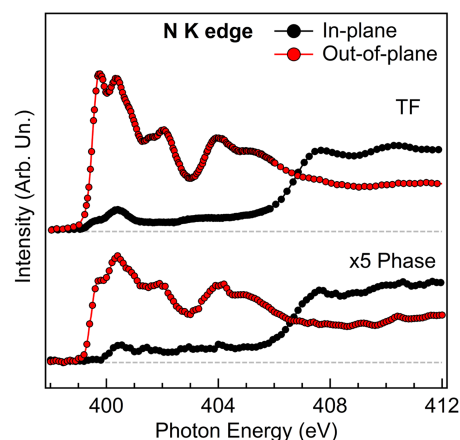


FIG. 2. N K absorption edges of MnPc/Au(110) for both in-plane (black) and out-of-plane (red) linearly polarized radiation of a thick MnPc molecular film (upper spectrum) and of a $\times 5$ phase (lower spectrum).

Au(110) surface at the sub-SL phase.^{23,27} The linear dichroism, preserved in the TF configuration (Fig. 2, top panel), is the result of the flat-lying growth of the subsequent molecular layers.

Despite the similar lineshapes at low and high MnPc coverage, there are slight differences that are worth noting: the total intensity of the first π^* multiplet (399.5 and 400.5 eV) is reduced in the spectrum at low coverage, compared to one of the MnPc TFs, and the relative intensity of the multiplet features with π^* symmetry further changes in the $\times 5$ phase due to the fairly strong molecule-substrate interaction, also deduced by scanning tunneling spectroscopy measurements in Ref. 22. Indeed, both effects pinpoint to a charge depletion from these orbitals at increasing molecular coverage, i.e., when the hybridization with the substrate is progressively weakened. The evolution of the N absorption peaks, evident in MnPc, is faint for FePc and absent for CoPc and CuPc chains adsorbed on the Au(110) surface.^{23,27} This symmetry breaking can be attributed to the occupancy of $3d_{\pi}$ empty molecular orbitals of MnPc, originated by the d_{xz} and d_{yz} states partially hybridized with the N- p orbitals in the isoindole sites.

B. MnPc on Au(110): Electronic state evolution as a function of molecular coverage

In order to unravel the interaction channels related to the Mn- d orbitals, X-ray absorption spectroscopy (XAS) measurements at the Mn L_3 edge at different molecular coverage are reported in Fig. 3(a), measured with the electric field of the incoming linearly polarized X-rays oriented parallel and perpendicular to the molecular plane. As previously proved by the N K-edge XAS, the MnPc molecules are lying flat on the Au channels. Hence, the X-ray search-light-like effect at the L_3 edge can distinguish between $3d$ orbitals with a predominant in-plane and out-of-plane orientation.

The MnPc thick film L_3 absorption edge, reported in Fig. 3(a), shows three distinct multiplet features for the in-plane polarization, located at around 639.7 eV, 640.9 eV, and 642.7 eV. The out-of-plane features are less structured presenting a weak shoulder at 640.0 eV and a more intense and broader structure at around 641.0 eV. Similar X-ray absorption spectroscopy spectra have been observed on MnPc molecular films grown on different substrates,^{14,28} with subtle variations due to the different thickness/morphology of the films. The most accepted ground state (GS) configuration for a MnPc molecule is a $4E_g$ symmetry with a $S = \frac{3}{2}$ spin state resulting from the $b_{2g}/d_{xy}^1, e_g/d_{xz+yz}^3, a_{1g}/d_{z^2}^1, b_{1g}/d_{x^2+y^2}^0$ configuration.^{10,29–32} However, the energy distance between different GS configurations is relatively small, being in the order of 0.1–0.3 eV.^{29,31,32} XAS measurements at the Mn $L_{2,3}$ are in favor to a $4E_g$ GS configuration as the L_3 intensity is fairly homogeneously distributed between the in-plane (rising from transitions to d_{xy} , d_{xz+yz} , and, at higher energies, $d_{x^2+y^2}$ orbitals) and out-of-plane (due to absorption towards d_{xz+yz} and d_{z^2} states) spectra, indicating an almost equal spectral weight of empty states with such orientations. An unambiguous attribution of the absorption features and one to one correspondence to molecular empty

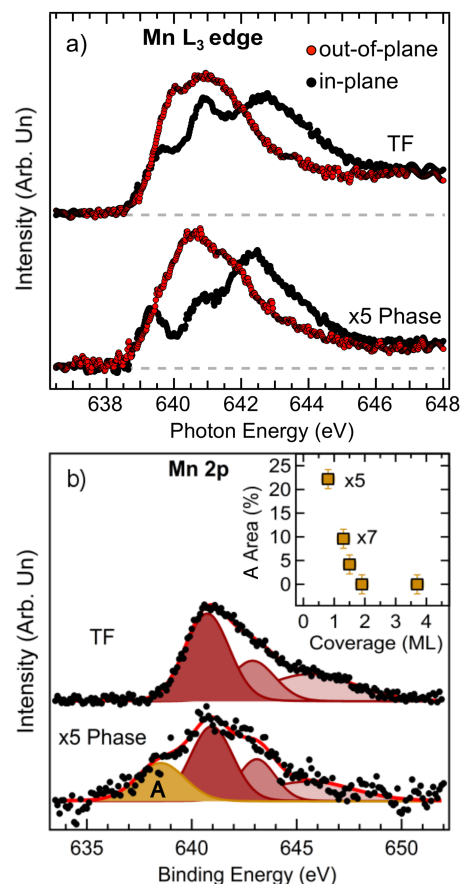


FIG. 3. (a) Mn L_3 X-ray absorption and (b) Mn $2p_{3/2}$ photoemission spectra for a MnPc TF and for the MnPc $\times 5$ phase. Inset: normalized area of the interaction feature (A) as a function of the molecular density.

levels are hindered by multiplet configuration and correlation effects.

The MnPc ordered SL on the Au(110) surface with a $\times 5$ phase presents striking changes to the L_3 lineshape. The broad lineshape of the out-of-plane L_3 edge spectrum [Fig. 3(a), red line] changes with respect to the MnPc TF, indicating hybridization of the out-of-plane Mn d -orbitals with the Au(110) substrate. The in-plane spectrum evolution of MnPc at the interface [Fig. 3(a), black lines] presents a richer phenomenology. In the lowest coverage phase with a $\times 5$ symmetry reconstruction, we can observe that the three previously described features are still visible but with a different intensity ratio with respect to the MnPc thick molecular film. In particular, the feature at 640.9 eV is strongly decreased, while the other two structures are reduced but preserve their relative intensity. This evolution suggests a participation of the planar $3d$ orbitals in the interaction process. The charge transfer from the substrate to the MnPc molecule, responsible of the XAS intensity damping as a result of the molecular orbitals occupation, is more effective at the low coverage phase, as observed for other MPcs adsorbed on Au(110).^{21,33} These observations suggest a redistribution of the $3d$ metal energy states and a consequent symmetry-breaking of the ground state, that can rearrange and mix with other low-energy configurations.²⁸ Mixed GS configurations as well as transitions between different GSs can occur either when the molecule is supported on a surface, as a result of hybridization with the substrate electronic

states, or in its crystalline form due to the interaction between neighbouring molecules via the pyrrole N atoms.^{30,32,34} The L_3 evolution seems to suggest that in the $\times 5$ phase, the interaction with the Au(110) surface is mediated by both in-plane b_{2g}/d_{xy} and out-of-plane oriented e_g/d_{xz+yz} and a_{1g}/d_{z^2} 3d orbitals that are close to the Fermi level.^{29,32} At increasing coverage, the interaction with the in-plane distributed orbitals becomes less favorable, while the orbitals protruding from the molecular center are still experiencing a strong charge transfer from the substrate.

In order to clarify the occurrence of a definite charge transfer and/or molecule-substrate orbital intermixing involving the Mn central metal atom, XPS measurements of the Mn 2p core level were carried out. Since the Mn 2p core level lies on Au 4p_{1/2}, a delicate background-subtraction procedure has been performed to remove the predominant contribution from the substrate. In particular, the spectrum of the freshly cleaned Au(110) surface was smoothed following a fourth order Savitzky-Golay algorithm and it was normalized to the calibrated molecular coverage. The results of such analysis is reported in Fig. 3(b) for the $\times 5$ phase and a MnPc TF. The asymmetric lineshape of the Mn 2p core level results from the presence of multiple components, due to the fourfold split ($m_j = -\frac{3}{2}, -\frac{1}{2}, \frac{1}{2}, \frac{3}{2}$) 2p_{3/2} level. The Zeeman splitting has been partially resolved with two Gaussian peaks, located at 640.9 eV and 643.1 eV, while a broader satellite is located at a higher binding energy, 645.5 eV. For the $\times 5$ phase, this fitting procedure cannot account for the extra spectral weight at lower binding energies, thus another Gaussian peak, located at 638.3 eV, was considered. The presence in the $\times 5$ phase of an extra component located at lower binding energies, labeled as A in Fig. 3(b), is a further indication of a central metal ion-mediated molecule-substrate interaction.^{35–40} Indeed, we noticed a sudden decrease of the A feature intensity at increasing molecular coverage [inset of Fig. 3(b)] just after the completion of the first SL. This suggests an interface-related electronic interaction, with a charge transfer from the Au metallic states to the Mn central metal atoms.

The MnPc adsorption on Au(110) induces a charge redistribution, modifying the fourfold symmetry of the molecular orbitals located on the Mn metal centers, involving in-plane and out-of-plane d -orbitals of the central metal atoms. Re-hybridization involves the N isoindole neighbors by the intermixing of e_g/d_{xz+yz} molecular states. The more complex MnPc–Au interaction process, with respect to the other MPcs, is justified by an orbital intermixing involving both in-plane and out-of-plane orbitals. Indeed, the main channel of charge transfer for CoPc and FePc is associated with the singly occupied a_{1g}/d_{z^2} state hybridized with the underlying Au states while the interaction is almost negligible for other MPcs with almost filled out-of-plane d states, like CuPc, NiPc, and ZnPc.¹⁹

To shed light on the evolution of the occupied states at the MnPc/Au(110) interface, high-resolution valence band photoemission spectroscopy measurements were performed at increasing molecular coverage, as reported in Fig. 4(a). The Au(110) clean surface spectrum is characterized by a broad set of features associated with the surface-projected spectral density such as the feature labeled as SS (Surface State), being

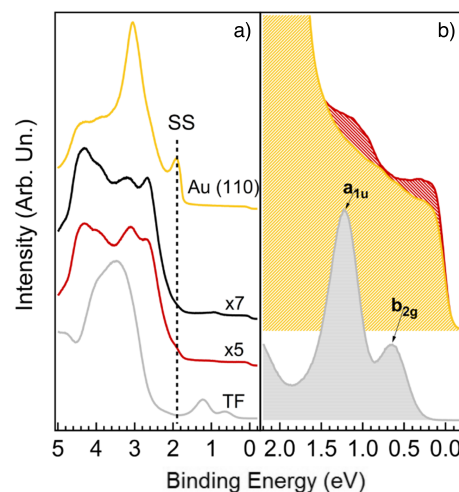


FIG. 4. (a) Normal-emission valence band photoemission spectra (photon energy of $h\nu = 21.218$ eV) for the different MnPc coverage phases on Au(110) and (b) close-up in the 0–2 eV binding energy region. All the spectra have been integrated over a 16° angular window centered at normal emission along the [001] direction.

a surface-localized electronic state. In the early stages of the molecular deposition, an intensity damping of the surface features can be observed, and the SS state is totally quenched only at the completion of the $\times 7$ phase. When a thick MnPc film is deposited, the molecular-states contribution to the spectral density becomes dominant. The MnPc TF spectrum is characterized by two main features in the 0–2 eV region: the HOMO state at 0.6 eV, associated with the b_{2g} orbital, mostly localized on the Mn atoms and with a dominant d_{xy} symmetry,³² and the HOMO-1 level at 1.2 eV, which can be assigned to the a_{1u} orbital, localized on the pyrrole ring.³² The comparison with other MPcs TF valence-band photoemission spectra evidences that the a_{1u} symmetry state is almost unaffected by the metal configuration, while a progressive shift to lower binding energies of the b_{2g} state as a function of the lower 3d metal occupation is observed.¹⁹

At lower molecular coverage, the identification of the different contributions is less straightforward as the hybridization of the molecular states with the substrate becomes dominant. For the $\times 5$ phase [full red curve in Fig. 4(b)] in the energy region below the Fermi level, we can identify two structures: one located at around 0.2 eV below the Fermi level and a second broader structure at 1.1 eV. This second feature persists at the completion of the SL and progressively develops into the a_{1u} peak of the TF as the molecular coverage is increased.

The presence of different interaction states close to the Fermi level can be related to 3d metal states involved in the interaction process, as previously observed with spatially resolved spectroscopic measurements.²² Indeed, MPcs with an open 3d shell (e.g., FePc and CoPc) are prone to form interface states when deposited on the Au(110) surface, due to the charge transfer from the substrate electrons to the 3d metal orbitals.^{19,27} Recently, Mn-related interface states have been observed for MnPc adsorbed on Au(111) and Ag(111) substrate.^{14,18} A similar 3d resonant enhancement of the spectral density close to the Fermi level was already

observed for a monolayer of FePc adsorbed on Au(100) and Ag(111), ascribed to a charge transfer between the molecular 3d open shell and the substrate.⁴¹ In the MnPc case, this effect becomes even more evident as the complex electronic structure of a 3d partially filled shell can open a higher number of interaction channels mediated by the 3d-metal orbitals. Furthermore, a Kondo state on the $\times 5$ phase has been unveiled for the FePc/Au(110) system, with an e_g symmetry parent state, implying a quenching of the magnetic moment of the molecule.⁴² The occurrence of a Kondo state has also been observed for MnPc adsorbed on Ag(001),⁴³ Pb(111),⁴⁴ and Au(111).⁴⁵ The coexistence of a Kondo channel, with e_g parent states, cannot be excluded for the MnPc chains assembled on Au(110) in the $\times 5$ phase, but the intensity of the broad spectral density close to the Fermi level, independent on the temperature, can be mainly ascribed to the charge transfer from the substrate electrons to the 3d metal orbitals.

III. CONCLUSIONS

MnPc deposited on the Au(110) surface induces a self-templating effect of the metal surface, driving the self-assembly of planar molecules from 1D chains to long-range ordered 2D reconstructed structures.

The monotone decrease of the work function can be understood in a donation/back-donation process, where the polarization of the organic macrocycles lowers the work function, while the empty metal states act as acceptor, thus receiving the back-donated electron and counterbalancing the work function reduction, in analogy with other 3d metal phthalocyanines adsorbed on metals.

The MnPc adsorption on Au(110), with a donation/back-donation process, induces re-hybridization of the electronic states localized on the central metal atom as well as on the organic macrocycle, favoring a rearrangement of the charge density and the modification of the isolated MnPc orbital structure. The interaction process for MnPc has been attributed to the more complex electronic configuration expected for a partially occupied 3d shell, together with the almost degenerate energy of the ground state and first excited states that are expected to be mixed by the interaction with the Au(110) substrate.

ACKNOWLEDGMENTS

The authors acknowledge the Aloisa beamline staff for the experimental support during the beamtime. This work was supported by Ateneo fund of Sapienza University of Rome.

¹J. Barth, *Annu. Rev. Phys. Chem.* **58**, 375 (2007).

²M. G. Betti, P. Gargiani, C. Mariani, R. Biagi, J. Fujii, G. Rossi, A. Resta, S. Fabris, S. Fortuna, X. Torrelles, M. Kumar, and M. Pedio, *Langmuir* **28**, 13232 (2012).

³L. Gavioli, M. Fanetti, M. Sancrotti, and M. G. Betti, *Phys. Rev. B* **72**, 035458 (2005).

⁴A. Cornia and P. Seneor, *Nat. Mater.* **16**, 505 (2017).

⁵J. Bartolomé, C. Monton, and I. K. Schuller, in *Molecular Magnets*, edited by J. Bartolomé, F. Luis, and J. F. Fernández (Springer-Verlag Berlin Heidelberg, 2014), Chap. 9, pp. 221–245.

⁶M. Hirokazu, O.-N. Hiroaki, and D. Yasuo, *Bull. Chem. Soc. Jpn.* **46**, 2724 (1973).

⁷K. Awaga and Y. Maruyama, *Phys. Rev. B* **44**, 2589 (1991).

⁸C. G. Barraclough, R. L. Martin, S. Mitra, and R. C. Sherwood, *J. Chem. Phys.* **53**, 1638 (1970).

⁹H. Yamada, T. Shimada, and A. Koma, *J. Chem. Phys.* **108**, 10256 (1998).

¹⁰T. Kataoka, Y. Sakamoto, Y. Yamazaki, V. R. Singh, A. Fujimori, Y. Takeda, T. Ohkuchi, S.-I. Fujimori, T. Okane, Y. Saitoh, H. Yamagami, and A. Tanaka, *Solid State Commun.* **152**, 806 (2012).

¹¹F. Evangelista, A. Ruocco, R. Gotter, A. Cossaro, L. Floreano, A. Morgante, F. Crispoldi, M. G. Betti, and C. Mariani, *J. Chem. Phys.* **131**, 174710 (2009).

¹²T. S. Ellis, K. T. Park, S. L. Hulbert, M. D. Ulrich, and J. E. Rowe, *J. Appl. Phys.* **95**, 982 (2004).

¹³M. Toader, P. Shukryna, M. Knupfer, D. R. T. Zahn, and M. Hietschold, *Langmuir* **28**, 13325 (2012).

¹⁴F. Petraki, H. Peisert, F. Latteyer, U. Aygöl, A. Vollmer, and T. Chassé, *J. Phys. Chem. C* **115**, 21334 (2011).

¹⁵P. Gargiani, G. Rossi, R. Biagi, V. Corradini, M. Pedio, S. Fortuna, A. Calzolari, S. Fabris, J. C. Cezar, N. B. Brookes, and M. G. Betti, *Phys. Rev. B* **87**, 165407 (2013).

¹⁶S. Stepanow, P. S. Miedema, A. Mugarza, G. Ceballos, P. Moras, J. C. Cezar, C. Carbone, F. M. F. de Groot, and P. Gambardella, *Phys. Rev. B* **83**, 220401 (2011).

¹⁷S. Stepanow, A. Mugarza, G. Ceballos, P. Moras, J. C. Cezar, C. Carbone, and P. Gambardella, *Phys. Rev. B* **82**, 014405 (2010).

¹⁸F. Petraki, H. Peisert, P. Hoffmann, J. Uihlein, M. Knupfer, and T. Chassé, *J. Phys. Chem. C* **116**, 5121 (2012).

¹⁹P. Gargiani, M. Angelucci, C. Mariani, and M. G. Betti, *Phys. Rev. B* **81**, 085412 (2010).

²⁰F. Evangelista, A. Ruocco, D. Pasca, C. Baldacchini, M. G. Betti, V. Corradini, and C. Mariani, *Surf. Sci.* **566-568**, 79 (2004).

²¹S. Fortuna, P. Gargiani, M. G. Betti, C. Mariani, A. Calzolari, S. Modesti, and S. Fabris, *J. Phys. Chem. C* **116**, 6251 (2012).

²²M. Topyła, N. Néel, and J. Kröger, *Langmuir* **32**, 6843 (2016).

²³L. Floreano, A. Cossaro, R. Gotter, A. Verdini, G. Bavdek, F. Evangelista, A. Ruocco, A. Morgante, and D. Cvetko, *J. Phys. Chem. C* **112**, 10794 (2008).

²⁴W. Gao and A. Kahn, *J. Phys.: Condens. Matter* **15**, S2757 (2003).

²⁵V. De Renzi, R. Rousseau, D. Marchetto, R. Biagi, S. Scandolo, and U. del Pennino, *Phys. Rev. Lett.* **95**, 046804 (2005).

²⁶M. G. Betti, A. Kanjilal, C. Mariani, H. Vázquez, Y. J. Dappe, J. Ortega, and F. Flores, *Phys. Rev. Lett.* **100**, 027601 (2008).

²⁷M. G. Betti, P. Gargiani, R. Frisenda, R. Biagi, A. Cossaro, A. Verdini, L. Floreano, and C. Mariani, *J. Phys. Chem. C* **114**, 21638 (2010).

²⁸T. Kroll, R. Kraus, R. Schönfelder, V. Y. Aristov, O. V. Molodtsova, P. Hoffmann, and M. Knupfer, *J. Chem. Phys.* **137**, 054306 (2012).

²⁹M.-S. Liao, J. D. Watts, and M.-J. Huang, *Inorg. Chem.* **44**, 1941 (2005).

³⁰Y. Kitaoka, T. Sakai, K. Nakamura, T. Akiyama, and T. Ito, *J. Appl. Phys.* **113**, 17E130 (2013).

³¹B. E. Williamson, T. C. VanCott, M. E. Boyle, G. C. Misener, M. J. Stillman, and P. N. Schatz, *J. Am. Chem. Soc.* **114**, 2412 (1992).

³²I. E. Brumboiu, R. Totani, M. de Simone, M. Coreno, C. Grazioli, L. Lozzi, H. C. Herper, B. Sanyal, O. Eriksson, C. Puglia, and B. Brena, *J. Phys. Chem. A* **118**, 927 (2014).

³³M. G. Betti, P. Gargiani, C. Mariani, S. Turchini, N. Zema, S. Fortuna, A. Calzolari, and S. Fabris, *J. Phys. Chem. C* **116**, 8657 (2012).

³⁴S. Stepanow, A. L. Rizzini, C. Krull, J. Kavich, J. C. Cezar, F. Yakhov-Harris, P. M. Sheverdyaeva, P. Moras, C. Carbone, G. Ceballos, A. Mugarza, and P. Gambardella, *J. Am. Chem. Soc.* **136**, 5451 (2014).

³⁵C. Isvoranu, B. Wang, K. Schulte, E. Ataman, J. Knudsen, J. N. Andersen, M. L. Bocquet, and J. Schnadt, *J. Phys.: Condens. Matter* **22**, 472002 (2010).

³⁶L. Massimi, M. Angelucci, P. Gargiani, M. G. Betti, S. Montoro, and C. Mariani, *J. Chem. Phys.* **140**, 244704 (2014).

³⁷M. Schmid, J. Zirzmeier, H.-P. Steinrück, and J. M. Gottfried, *J. Phys. Chem. C* **115**, 17028 (2011).

³⁸M. Schmid, A. Kaftan, H.-P. Steinrück, and J. M. Gottfried, *Surf. Sci.* **606**, 945 (2012).

³⁹G. Avvisati, P. Mondelli, P. Gargiani, and M. G. Betti, *Appl. Surf. Sci.* (to be published).

- ⁴⁰G. Avvisati, S. Lisi, P. Gargiani, A. Della Pia, O. De Luca, D. Pacilé, C. Cardoso, D. Varsano, D. Prezzi, A. Ferretti, and M. G. Betti, *J. Phys. Chem. C* **121**, 1639 (2017).
- ⁴¹F. Petraki, H. Peisert, U. Aygöl, F. Latteyer, J. Uihlein, A. Vollmer, and T. Chassé, *J. Phys. Chem. C* **116**, 11110 (2012).
- ⁴²P. Gargiani, M. G. Betti, A. Taleb Ibrahimi, P. Le Fèvre, and S. Modesti, *J. Phys. Chem. C* **120**, 28527 (2016).
- ⁴³J. Kügel, M. Karolak, A. Krönlein, J. Senkpiel, P.-J. Hsu, G. Sangiovanni, and M. Bode, *Phys. Rev. B* **91**, 235130 (2015).
- ⁴⁴K. J. Franke, G. Schulze, and J. I. Pascual, *Science* **332**, 940 (2011).
- ⁴⁵L. Liu, K. Yang, Y. Jiang, B. Song, W. Xiao, L. Li, H. Zhou, Y. Wang, S. Du, M. Ouyang, W. A. Hofer, A. H. Castro Neto, and H.-J. Gao, *Sci. Rep.* **3**, 1210 (2013).